Short Papers

A Waveguide Polarization Controller

Kamal Sarabandi

Abstract—**In this paper a novel waveguide polarizer is introduced that does not require rotary joints and the frequency of operation can easily be adjusted by a few set screws. In this method the degenerate eigenvalues of a circular waveguide are separated by deforming the waveguide cross section slightly. In order to generate a desired polarization, the orientation angle of the deformation point with respect to the polarization of the incident wave can be adjusted using a rotary roller mechanism concentric with the circular waveguide. Analysis of the problem based on the finite element method and an approximate analytical method is given. A prototype model at 34.5 GHz is built and tested. Experimental results shows excellent agreement with the theoretical prediction.**

I. INTRODUCTION

Polarization agility in a military or remote sensing radar enhances the ability of the radar system in detection and measurement of a feature of interest in a radar scene [1]. Traditionally, the desired polarization in a transmitter is generated by employing one or two dielectric septum polarizers or corrugated dielectric wave-plates [2]. In the dielectric septum polarizer, a thin dielectric sheet of quarter-wavelength long is placed longitudinally in a circular waveguide which introduces a $\pi/2$ phase difference between two modes in space quadrature. Since the output polarization of a septum polarizer depends on the relative orientation of the dielectric septum with respect to the polarization of the incident wave, waveguide rotary joints are required to generate a set of desired polarizations. Although a choke is usually used with a waveguide rotary joint to reduce reflection at the interface of the flanges, the VSWR as a function of twist angle can be as high as 1.4 at X-band [3]. The somewhat random phase and amplitude variations as a function of twist angle caused by the rotary joint, degrade the performance of the polarizer.

An alternative way of controlling the polarization at millimeter and submillimeter wavelengths is to place an anisotropic (or corrugated) dielectric plate in front of the transmitter [4]. Since the dielectric wave-plate is illuminated by a spherical phase front, the axial ratio degrades away from the bore sight. Problems such as interaction of the corrugated dielectric wave-plate with the antenna and different attenuation for the components of the wave parallel and perpendicular to the optical axis degrades the polarization purity of the device.

It is shown that a squeezed rectangular waveguide can be used as a phase shifter [2], [5]. Based on this idea, design and analysis of a squeezed circular waveguide polarizer is presented. This polarizer does not require rotary joints and its center frequency can easily be adjusted by set screws.

II. THEORETICAL ANALYSIS

In this section theoretical analysis of squeezed waveguide polarizers is considered. The analysis involves two steps: 1) the mechanical and 2) electrical design consideration of a pinched cylindrical waveguide. In the mechanical analysis the objective is determination of the cross section geometry of the pinched cylinder and in the electrical analysis determination of the first two eigenvalues (cutoff frequencies) of the deformed waveguide is of interest.

Manuscript received July 6, 1993; revised February 7, 1994.

The author is with the Radiation Laboratory, Department of Electrical Engineering and Computer Science, The University of Michigan, Ann Arbor, MI 48109-2122 USA.

IEEE Log Number 9404634.

Fig. 1. Mechanical design of the squeezed waveguide polarizer (a prototype at Ka-band).

A. Mechanical Analysis

Fig. 1 shows the mechanical design of the rotatable waveguide squeezer. Two thick circular metallic disks are positioned concentric with the waveguide axis at each end of the waveguide section. Each concentric disk is supported over the waveguide surface by a bearing which facilitates rotation of the disk around the circular waveguide. The concentric disks are connected to each other by two shafts parallel to the axis and placed on opposite sides of the waveguide. The shafts are free to slide up and down in radial slots machined in the concentric disks. These shafts are the axes of two long roller bearings that are pinching the circular waveguide along two opposite lines parallel to the waveguide axis as shown in Fig. 1. The radial distance of the two osculating lines from the waveguide axis can be adjusted by the set screws, thereby the circular waveguide can be deformed to achieve the desired mode separation. In tuning the mode separation using the set screws, one must be careful not to exceed displacements outside the elastic region of the waveguide tubing.

The property of material, wall thickness, length of the osculating line (pinched section), and the inner radius of the waveguide are the influential parameters for proper mechanical design of the squeezed waveguide polarizer. The inner dimension of the circular waveguide is determined by the frequency of operation, thus is not a free parameter in mechanical design. The phase difference between the two orthogonal modes is proportional to the displacement of the waveguide wall from its normal configuration. Therefore in order to

0018–9480/94$04.00 © 1994 IEEE

get a larger phase difference for a given length of osculating line, the waveguide material must be chosen such that the ratio of the yield stress (S_y) to the Young's modulus of elasticity (E) is maximum amongst all possible alloys. Referring to a table of properties of metals [6], it can be seen that alloys of beryllium copper have the largest yield stress (as high as 175 Ksi) while their modulus of elasticity is reasonably low (around 18 Mpsi). Aside from its elastic property, beryllium copper has other properties suitable for this design such as strength, corrosion resistance, and high electrical conductivity.

Structural analysis of the pinched cylinder is required to obtain the stress distribution and the cross section deformation. The stress distribution in the waveguide wall is required to assure that the stress does not exceed the yield stress of the material. For this problem a finite element code (I-DEAS) was used to calculate the stress distribution and cross section deformation. It was found that the maximum stress is at the edge of the osculating lines and is almost linearly proportional to the thickness as long as $\tau/r \ll 1$. It was also found that for thin shells the cross section of the deformed waveguide is almost elliptical when the relative displacement ($\Delta r/r$) is under 7%. It is better to keep the displacement under 5% and achieve the desired phase shift by adjusting the length of the osculating line because the maximum stress increases rapidly with increasing displacement.

B. Numerical Solution

The finite element method offers an efficient numerical procedure in the calculation of the eigenvalues of a waveguide with arbitrary cross section [7]. This technique is well-known and here only a brief discussion of the method is outlined. For homogeneously-filled waveguides the longitudinal component of the electric (TM case) or magnetic (TE case) field, denoted by ψ, satisfies the homogeneous Helmholtz's equation $(\nabla^2 + K_c^2)\psi = 0$, where K_c is the cutoff wave number. It is shown that the solution to the Helmholtz's equation minimizes the following functional [8]

$$F(\psi) = \frac{\int\int_S \nabla\psi \cdot \nabla\psi \mathrm{d}s}{\int\int_S \psi^2 \mathrm{d}s} \tag{1}$$

and the minimum is equal to the smallest eigenvalue $\lambda = K_c^2$. To find the minima of the functional the eigenfunction ψ is approximated by a piecewise linear function. In this approximation the cross section of the waveguide is discretized into small triangular elements with unknown values of ψ at each node of the elements. Substituting the piecewise linear function into the functional (1) and searching for the minima by setting $\frac{\delta}{\delta\psi_j^e} = 0$, the following matrix equation is obtained

$$\mathbf{A}\Psi = K_c^2 \mathbf{B}\Psi. \tag{2}$$

Equation (2) is recognized as the generalized eigenvalue problem which can be solved for K_c numerically using a standard method [9].

C. Asymptotic Solution

As was discussed in the mechanical design section a slightly pinched circular cylinder deforms into an almost elliptical cylinders. The degenerate eigenvalues of the circular waveguides get separated into the so called even and odd modes of elliptical waveguides. The analytical solution for the cutoff frequencies and the associated phase constants of elliptical waveguides is known and therefore the phase difference between the dominant even and odd modes can be calculated [10]. In this section a simple closed form expression for the cutoff frequencies of the first two dominant modes of the almost circular waveguide is obtained.

Consider the elliptic coordinate system (μ, η, z) with parameter ρ. In this coordinate system, surfaces of constant μ specify confocal elliptical cylinders with ρ being half the distance between the foci. For the squeezed cylinder of radius r, represent the displacement of the surface at the pinched point by Δr. In this case the major and minor axes of the ellipse are $2(r + \Delta r)$ and $2(r - \Delta r)$ respectively. It is assumed that the relative displacement $\delta = \Delta r/r \ll 1$. The interfocal distance 2ρ in terms of relative displacement δ and radius of the original cylinder r is given by

$$\rho = 2r\sqrt{\delta} \tag{3}$$

and $\mu_0 = \tanh^{-1}[(1-\delta)/(1+\delta)]$ specifies the surface of the ellipse. The fields inside the elliptical cylinder may be expanded in terms of elliptical harmonic functions also known as angular $(S_m^e(\eta), S_m^o(\eta))$ and radial $(R_m^e(\mu), R_m^o(\mu))$ Mathieu functions [12]. Since the dominant mode of a circular waveguide is TE_{11}, the first two modes in the almost circular elliptical waveguide are TE_{11}^e and TE_{11}^o. To obtain an approximate solution for the cutoff frequencies of these modes, expansions of the radial Mathieu functions of the first kind in terms of Bessel functions are needed. For odd orders of the radial Mathieu functions, these expansions are given by [11]

$$R_{2m+1}^e(\mu, q) = \frac{S_{2m+1}^{e\prime}(\pi/2, q)}{\sqrt{q} A_1^{(2m+1)}} \times \sum_{k=0}^{\infty} (-1)^{k+1} A_{2k+1}^{(2m+1)} J_{2k+1}(2\sqrt{q}\cosh\mu) \tag{4}$$

$$R_{2m+1}^o(\mu, q) = \frac{S_{2m+1}^{o\prime}(0, q)}{\sqrt{q} B_1^{(2m+1)}} \times \sum_{k=0}^{\infty} B_{2k+1}^{(2m+1)} J_{2k+1}(2\sqrt{q}\sinh\mu) \tag{5}$$

where $q = \frac{1}{4}K_c^2\rho^2 = K_c^2 r^2 \delta$ and K_c is the cutoff wave number ($K_c = 2\pi/\lambda$). The coefficients $A_{2k+1}^{(2m+1)}$ and $B_{2k+1}^{(2m+1)}$ in (4) and (5) are functions of q. The first even and odd modes correspond to $m = 0$ in the above equations. Since $q \ll 1$, a power series expansion of the angular Mathieu functions can be used in (4) and (5). Keeping the terms up to the first order in q, after some tedious algebraic manipulation it can be shown that

$$R_1^e(\mu, q) \approx \frac{1}{\sqrt{q}}\left[1 + \frac{3q}{8} J_1(2\sqrt{q}\cosh\mu) + \frac{q}{8} J_3(2\sqrt{q}\cosh\mu)\right] \tag{6}$$

$$R_1^o(\mu, q) \approx \frac{1}{\sqrt{q}}\left[1 - \frac{3q}{8} J_1(2\sqrt{q}\sinh\mu) - \frac{q}{8} J_3(2\sqrt{q}\sinh\mu)\right]. \tag{7}$$

For TE waves the boundary condition requires that

$$\frac{d}{d\mu} R_1^{e,o}(\mu, q) = 0 \qquad \text{at} \quad \mu = \mu_0. \tag{8}$$

The solution of these equations for q give the cutoff frequencies for the even and odd TE_{1n} modes. The dominant cutoff frequencies of the slightly deformed circular waveguide are slightly different from that of the circular waveguide, thus to the first order in δ

$$K_c^{e,o} \approx k_c^0(1 + \kappa^{e,o}\delta)$$

where $k_c^0 = 1.841/r$ is the cutoff wave number for the circular waveguide. Substituting (6) and (7) into (8), noting that $\cosh\mu_0 = (1+\delta)/(2\sqrt{\delta})$ and $\sinh\mu_0 = (1-\delta)/(2\sqrt{\delta})$, and then expanding the Bessel functions in terms their Taylor series to the first order in δ, it can be shown that

$$K_c^e \approx k_c^0(1 - 0.9183\delta) \tag{9}$$

$$K_c^o \approx k_c^0(1 + 0.9183\delta). \tag{10}$$

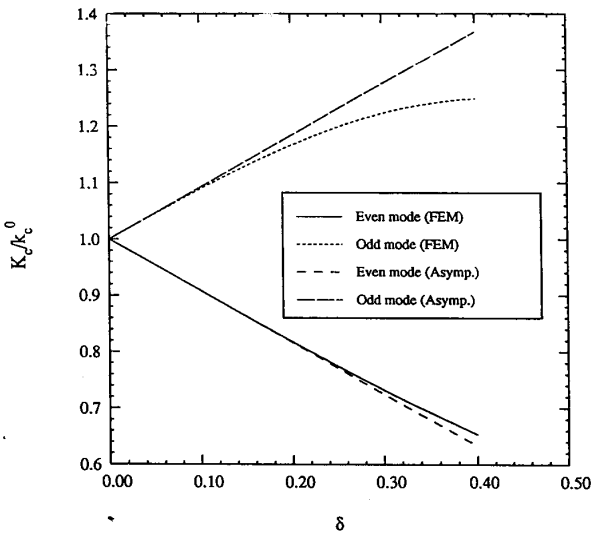

Fig. 2. First two cutoff wave number for an elliptical waveguide with axial ratio $\frac{1+\delta}{1-\delta}$ normalized to the dominant cutoff wave number of the circular waveguide ($\delta = 0$).

The cutoff wavenumbers given by (9) and (10) are comparered with those computed from the finite element code in Fig. 2. It can be seen that the asymptotic expression provides accurate results for values of δ as high as 10% for the odd mode and 20% for the even mode.

III. Experimental Results

A squeezed waveguide polarizer with a rotary mechanism was designed and tested at Ka-band frequencies. A cylindrical brass tube of inner diameter of 6.35 mm, outer diameter of 7.14 mm, and length 8 cm was chosen as the circular waveguide.

Knowing the cross section geometry and the displacement, the length of the osculating line can be determined from the required phase difference between the orthogonal modes. In practice, after setting the displacement to the nominal design value, fine adjustment may be required to get the precise desired phase shift between the orthogonal modes. To characterize the performance of the squeezed waveguide polarizer and fine-tune the phase shift, a new test setup is designed as shown in Fig. 3. An HP 8753C network analyzer is used as the sweeper and dual vector receiver. Since the operating frequency of the network analyzer is limited to 3 GHz, one up-converter and two down-converter (harmonic mixers) are used to extend the operating frequency to Ka-band. To increase the isolation between the up-converter and down-converters, bandpass filters were inserted in each branch of the power splitter.

The RF port of the up-converter is a rectangular waveguide oriented vertically and connected to the polarizer *via* a rectangular-to-circular waveguide adapter. The output of the polarizer is connected to an orthogonal mode transducer (OMT) with 40 dB isolation between the two orthogonal ports. The OMT at the output of the polarizer is oriented so that the orthogonal ports are at 45° with respect to the vertical direction.When the waveguide squeezer is unloaded, the polarizer does not modify the incident wave and the signals received in the A and B ports of the network analyzer should be identical. However, due to path length differences and variations in amplifier gains and mixer conversion losses, the received signal in the A and B ports are not identical. The measured A and B for the unsqueezed polarizer are used to find the differences between the two channels.

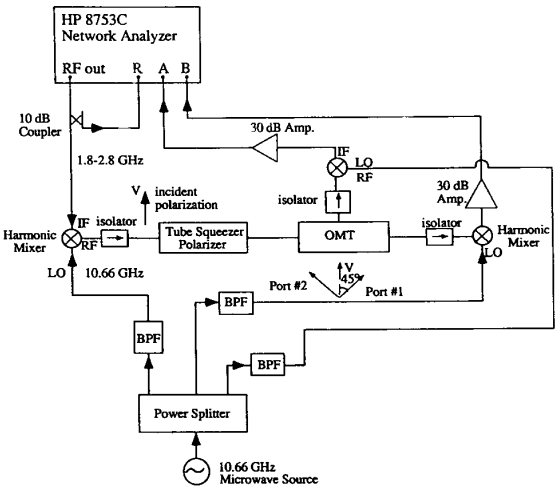

Fig. 3. Experimental setup for tuning and characterizing the prototype Ka-band squeezed waveguide polarizer.

Suppose $\hat{o}$ and $\hat{e}$ are two orthogonal unit vectors along the minor and major axes of the deformed waveguide and α is the angle between $\hat{o}$ and $\hat{v}$ (the polarization of the incident wave). Depending on the orientation angle α, the incident wave can excite both modes of propagations one with the electric field along the major axis, and the other one with the electric field along the minor axis of the ellipse. The component of the incident wave along the minor axis propagates more slowly than the component along the major axis which produces a phase difference ϕ between the two components. By decomposing the field at the output of the polarizer into two components along the ports of the OMT, it can be shown that the calibrated signal at the A and B ports of the network analyzer must satisfy

$$\frac{A}{B} = \frac{1 - e^{-j\phi}\tan(\alpha - 45)\cot(\alpha)}{\tan(\alpha - 45) + e^{-j\phi}\cot(\alpha)}. \tag{11}$$

In order to fine tune the polarizer for the desired ϕ, we notice that at the rotation angle $\alpha = 45°$, the phase difference between A and B signals is ϕ. In this experiment the rotary disk of the polarizer was engaged with a stepper motor to facilitate accurate positioning of the vectors $\hat{o}$ and $\hat{e}$ with respect to $\hat{v}$ within a fraction of a degree. For the prototype polarizer with $L = 1.9$ cm, $r = 0.317$ cm, and $f = 34.5$ GHz, the phase difference can be calculated from

$$\phi = L(k_z^e - k_z^o) \tag{12}$$

where k_z^e and k_z^o can be obtained from (9) and (10) respectively. To achieve a 90° phase shift a displacement of 5.5% is required which was verified experimentally. Fig. 4 compare the phase of the measured A/B to the expression (12) as a function of rotation angle. It can be seen that the agreement is excellent. In a separate measurement setup it was found that the return loss (S_{11}) of the polarizer was better than 40 dB.

IV. Conclusion

A new design for waveguide polarizers was presented. In this technique the degenerate eigenvalues of a circular waveguide are separated by deforming the cross section. The circular cylinder is pinched from the opposite sides so that the first two modes are in space quadrature. By choosing the length of the deformed section and the relative displacement a phase difference of $\pi/2$ between the two modes is introduced. The output polarization is controlled

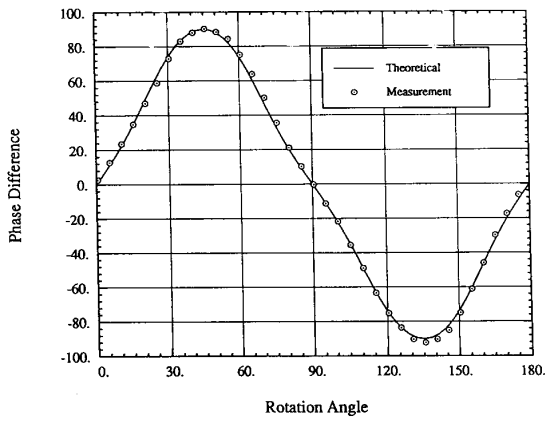

Fig. 4. The measured and calculated phase difference of the signals at the OMT output (A and B).

by a rotatable waveguide squeezer which facilitates rotation of the major axis of the deformed cross section with respect to the input polarization. The new polarizer does not require rotary joints and its center frequency can easily be adjusted using a few set screws. Analytical and numerical design procedures are presented and a prototype model at Ka-band is built and test.

REFERENCES

[1] D. Giuli, "Polarization diversity in radars," *Proc. IEEE*, vol. 74, pp. 245–269, Feb. 1986.
[2] A. F. Harvey, *Microwave Engineering*. New York: Academic Press, 1963.
[3] F. E. Ehlers, "Waveguide rotary joints," in G. L. Ragan, Ed., *Microwave Transmission Circuits*. Cambridge, MA: M.I.T. Radiation Laboratory Series, 1964.
[4] H. S. Krischbaum and L. Chen, "A method of producing broadband circular polarization employing an anisotropic dielectric," *IRE Trans. Microwave Theory Tech.*, vol. MMT-5, no. 3, pp. 199–203, July 1957.
[5] H. Schrank and G. Seck, "The spread-squeeze waveguide polarizer," *IEEE Antennas Propagat. Newsletter*, Oct. 1984.
[6] E. Oberg, F. D. Jones, and H. L. Horton, *Machinery's Handbook*. New York: Industrial Press, 1988.
[7] P. Silvester, "A general high-order finite-element waveguide analysis program," *IEEE Trans. Microwave Theory Tech.*, vol. MTT-17, Apr. 1969.
[8] J. W. Dettman, *Mathematical Methods in Physics and Engineering*. New York: Dover, 1988, pp. 149–169.
[9] J. H. Wilkinson, *The Algebraic Eigenvalue Problem*. New York: Oxford University Press, 1965.
[10] L. J. Chu, "Electromagnetic waves in elliptic hollow pipes of metal," *J. Appl. Phys.*, vol. 9, pp. 583–591, Sept. 1938.
[11] M. Abramowitz and I. A. Stegun, *Handbook of Mathematical Functions*. New York: Dover, 1972, pp. 722–746.

A Quasi-Optical Image Separation Scheme for Millimeter and Submillimeter Waves

Cheuk-yu Edward Tong and Raymond Blundell

***Abstract*—We propose a compact quasi-optical scheme to achieve image separation using two mixers. With this scheme, an image rejection ratio of better than 12 dB has been obtained over 25 GHz in W-band without any mechanical tuning. This diplexing scheme should find applications in remote sensing and radio astronomy.**

I. INTRODUCTION

At microwave frequencies, heterodyne receivers often incorporate single-side-band (SSB) mixers to either enhance conversion or to reject unwanted signals or noise. In the millimeter and submillimeter wave band, such techniques are still under development and are highly desirable. In the case of spectral line observations widely used in remote sensing and radio astronomy, image separation or image rejection is often an advantage [1]. Besides reducing confusion from lines present in the other side-band, a reduction in the system noise temperature is achieved by eliminating one of the side-bands.

A number of quasi-optical diplexer designs exist [2] and have been incorporated in millimeter and submillimeter systems for image rejection. Recently, a waveguide image separation receiver has been tested at 100 GHz and a quasi-optical version of this set-up has been proposed [3]. In this article, we present a very compact quasi-optical scheme to achieve image separation. Measurements made in the W-band confirm that image separation can be realized over a broad frequency range.

II. DIPLEXING SCHEME

The principle of operation of our scheme is well known: by introducing a 90-degree phase shift of the incident Local Oscillator (LO) drive between the two mixers, both side-bands can be separated on recombining the outputs of both mixers in a 90-degree hybrid circuit [4]. The details of our scheme are given in Fig. 1. Four wire grids functioning as polarizers [5] are arranged in a cross. Grids 3 and 4 are mounted on a translation stage, while grids 1 and 2 are fixed. Grids 1 and 3 act as 3-dB power dividers for the incident signal and LO beams respectively, while grids 2 and 4 are used as couplers to couple LO power into the signal paths of the mixers.

Referring to Fig. 2, consider the case when a vertically polarized (parallel to y-axis) signal beam is incident on grid 1. The polarizing action of the grid produces reflected and transmitted beams that are polarized at 45 degrees to the vertical. Mixers 1 and 2 are oriented so as to align to the polarizations of the reflected and transmitted beams respectively. Referring back to Fig. 1, grid 3 is used to split and rotate the polarization of the LO beam in a similar manner. The resultant reflected and transmitted beams are then weakly coupled to the mixers by grids 2 and 4. The loads asscoiated with the coupler grids are used to terminate the uncoupled LO power. Grid 5 is used to define the signal polarization. Added noise from the orthogonal polarization is minimized through the use of a cold termination as shown in Fig. 1. This scheme possesses an interesting feature: with proper orientation of the grid wires, it works not only when the signal

Manuscript received June 10, 1993; revised January 21, 1994.
The authors are with the Harvard-Smithsonian Center for Astrophysics, Cambridge, MA 02138.
IEEE Log Number 9404635.

0018-9480/94$04.00 © 1994 IEEE